J. Fluid Mech. (1966), *vol.* 25, *part* 2, *pp.* 321–330
Printed in Great Britain

Calculations of the development of an undular bore

By D. H. PEREGRINE
Department of Mathematics, University of Bristol

(Received 26 June 1965 and in revised form 22 November 1965)

If a long wave of elevation travels in shallow water it steepens and forms a bore. The bore is undular if the change in surface elevation of the wave is less than 0·28 of the original depth of water. This paper describes the growth of an undular bore from a long wave which forms a gentle transition between a uniform flow and still water. A physical account of its development is followed by the results of numerical calculations. These use finite-difference approximations to the partial differential equations of motion. The equations of motion are of the same order of approximation as is necessary to derive the solitary wave. The results are in general agreement with the available experimental measurements.

1. Introduction

A bore is a transition between different uniform flows of water. It is most easily studied in uniform, rectangular, open channels, and in this paper only such channels are considered. In its most common form, a bore is a turbulent, breaking zone of water whose length is a few times the depth of water. However, if the bore is weak, that is, if the change in water level is much less than the depth of water, the bore consists of a train of many waves whose wavelength is several times the depth of water. One method of forming a bore is to send a stream of water into an area of still water in a long, horizontal channel. The moving water has to be deeper than the still water in order to flow into it. If the transition between still water and the deeper water has initially a very gentle slope, the slope will steepen and form a bore. Experimental measurements by Favre (1935) show that undular bores form when the ratio of the change in level to the initial depth of water is less than 0·28. If this ratio is greater than 0·28 but less than 0·75 there are still undulations, but the first one at least is breaking (Binnie & Orkney 1955). For greater differences in depth there are no undulations.

One feature of undular bores is that the undulations are long compared with the depth of water. Thus, their formation may be looked at in terms of shallow-water theory. Keulegan & Patterson (1940) showed that the undulations measured by Favre had properties close to those of cnoidal waves. Cnoidal waves were first derived analytically by Korteweg & de Vries (1895) and are steady translational waves. Their limit as the wavelength is increased is the solitary wave. In the derivation of cnoidal waves two ratios ϵ and σ are assumed to be small; these are

$$\epsilon = \frac{\text{wave amplitude}}{\text{water depth}}, \quad \text{and} \quad \sigma = \frac{\text{water depth}}{\text{wavelength}}.$$

Wavelength is used here to mean the distance in which significant changes in surface height occur. There are equations for which ϵ need not be small. These are the finite-amplitude shallow-water equations, but they are not uniformly valid since they predict that, for waves entering still water, any forward-facing slope steepens until it is vertical; however, σ is then large and the assumption of small σ no longer holds. In this paper these equations and their solutions will be called Airy's theory since he first showed the effects of finite amplitude (for an account of the theory see Stoker 1957).

The variables used here are $\eta(x,t)$, the vertical displacement of the water surface from its original level, and $u(x,t)$, the mean horizontal velocity of the water. Non-dimensional variables are defined as follows:

$$\eta = \eta^*/h, \quad u = u^*/(gh)^{\frac{1}{2}}, \quad x = x^*/h, \quad t = t^*(g/h)^{\frac{1}{2}},$$

where * indicates a dimensional variable and h is the undisturbed depth of water, which is taken to be constant. The choice of u and η as independent variables is made since the continuity equation can then be written in the exact form

$$\frac{\partial \eta}{\partial t} + \frac{\partial}{\partial x}[(1+\eta)u] = 0. \tag{1}$$

If the flow is assumed to be irrotational with

$$\epsilon = O(\sigma^2) \ll 1,$$

which is appropriate for solitary and cnoidal waves, the momentum equation is

$$\frac{\partial u}{\partial t} + u\frac{\partial u}{\partial x} + \frac{\partial \eta}{\partial x} = \frac{1}{3}\frac{\partial^3 u}{\partial x^2\,\partial t} + O(\epsilon^2\sigma^3). \tag{2}$$

Note that scaling factors are not introduced with the non-dimensionalization, so that

$$u \sim \eta \sim \epsilon, \quad \text{and} \quad \partial/\partial x \sim \partial/\partial t \sim \sigma.$$

The third derivative on the right-hand side of (2) expresses the effect of the vertical acceleration of the water on the pressure. It is absent in Airy's theory where the pressure is taken to be hydrostatic.

Equations (1) and (2) may be simplified by assuming that waves only travel in one direction. If they travel in the $+x$-direction, it may be shown that

$$\frac{\partial u}{\partial t} + \frac{\partial u}{\partial x} + \tfrac{3}{2}u\frac{\partial u}{\partial x} = \frac{1}{6}\frac{\partial^3 u}{\partial x^2\,\partial t} + O(\epsilon^2\sigma^3), \tag{3}$$

and

$$\eta = u + O(\epsilon^2).$$

Korteweg & de Vries (1895) first investigated an equation like this by considering waves varying slowly when travelling against a uniform stream. For a recent derivation of these equations in which a slightly different velocity variable is used, see Broer (1964).

The only known analytical solutions of these equations are the solitary wave and cnoidal waves. These solutions are valid for all times, unlike Airy's theory, so that it is reasonable to suppose that these equations are uniformly valid in time if the initial conditions satisfy the assumptions made in their derivation.

Finite-difference methods were used to find numerical solutions of the equations corresponding to the development of an undular bore from an initial wave like that in figure 1.

The next section gives a physical account of the bore's initial growth. It is followed by sections on the numerical methods and the results of calculations. The fully developed bore is considered in the last section. The single equation (3) is referred to as I, and the two equations (1) and (2) as II.

2. Physical description

Consider a long shallow-water wave like that in figure 1. Suppose that the change in level is initially much less than one and that $\sigma^2 \ll \epsilon$. The wave steepens until σ^2 is no longer much less than ϵ. This phase of the motion is described well by Airy's theory and the pressure in the water is effectively hydrostatic. Once $\sigma^2 \sim \epsilon$, this is no longer so. The water surface between the two uniform levels is then sufficiently steep for the vertical acceleration of the water to affect the pressure significantly.

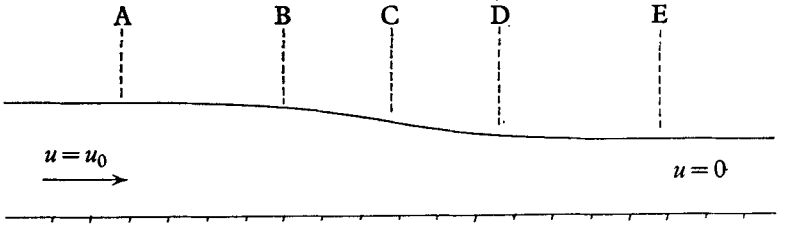

FIGURE 1. The initial wave.

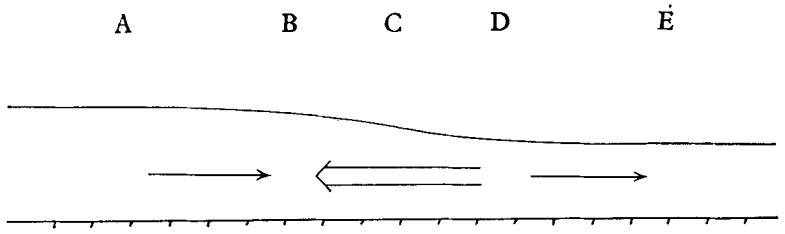

FIGURE 2. The extra horizontal pressure gradients due to the vertical acceleration of the water.

Suppose the wave in figure 1 has reached this state. The vertical acceleration of the water is upward between E and C. There, the pressure gradient downward beneath the surface must be greater than hydrostatic for this acceleration to occur. Similarly between C and A the downward pressure gradient must be less than hydrostatic since the water has a downward acceleration there. The greatest changes from hydrostatic pressure will occur at B and D, the points of maximum vertical acceleration (and of maximum surface curvature). The pressure beneath D is greater than hydrostatic and beneath B it is less; therefore the horizontal pressure gradients are affected and there is an extra horizontal pressure gradient from D to B. Similarly, there is a slight extra horizontal pressure gradient from D to E, and from A to B, as indicated in figure 2.

Thus compared with the change of profile expected from an assumption of hydrostatic pressure, that is, Airy's theory, these pressure gradients cause an extra elevation at B, a corresponding depression at D, a slight depression at A, and a slight elevation at E. This process continues and a sequence of waves is formed, which grow in amplitude until their tendency to steepen is just balanced by the horizontal pressure gradients due to the vertical acceleration of the water.

3. Numerical approximations

Equations I and II may be called parabolic-hyperbolic; all their characteristics are real but one pair are coincident. However, this is not important since the highest derivative is $O(\epsilon\sigma^3)$ and may be approximated in several different ways; for example, Long (1964) manipulates the equations so that all the characteristics are distinct. The type of the equations is relevant to the stability of numerical approximations.

For I the following straightforward finite-difference approximation was used:

$$\frac{u_{r,s+1}-u_{r,s}}{\Delta t}+(1+\tfrac{3}{2}u_{r,s})\frac{u_{r+1,s+1}-u_{r-1,s+1}+u_{r+1,s}-u_{r-1,s}}{4\Delta x}$$
$$=\frac{1}{6\Delta x^2\Delta t}(u_{r+1,s+1}-2u_{r,s+1}+u_{r-1,s+1}-u_{r+1,s}+2u_{r,s}-u_{r-1,s}), \quad (4)$$

where $u_{r,s}=u(r\Delta x, s\Delta t)$.

Solutions were calculated step by step in time; the values $u_{r,s}$ $(r=1,\ldots,n)$ and boundary values $u_{1,s+1}$, $u_{n,s+1}$ were used to find $u_{r,s+1}$. The solutions were stable and appeared to converge as Δx and Δt were reduced. In all except some preliminary calculations, Δx was taken equal to Δt, and will be referred to as Δ.

Straightforward finite-difference approximations for II are unstable and the following scheme was used. An approximation to the continuity equation was used to calculate a provisional value of η at the advanced time step, that is $\eta^*_{r,s+1}$. An approximation to the momentum equation then gave $u_{r,s+1}$, which was used in the continuity equation to obtain a corrected value of $\eta_{r,s+1}$.

The finite-difference equations used for II are as follows.

(i) The continuity equation to find $\eta^*_{r,s+1}$ is

$$\frac{\eta^*_{r,s+1}-\eta_{r,s}}{\Delta t}+[1+\tfrac{1}{2}(\eta^*_{r,s+1}+\eta_{r,s})]\frac{u_{r+1,s}-u_{r-1,s}}{2\Delta x}+u_{r,s}\frac{\eta_{r+1,s}-\eta_{r-1,s}}{2\Delta x}=0. \quad (5)$$

(ii) The momentum equation to find $u_{r,s+1}$ is

$$\frac{u_{r,s+1}-u_{r,s}}{\Delta t}+u_{r,s}\frac{u_{r+1,s+1}-u_{r-1,s+1}+u_{r+1,s}-u_{r-1,s}}{4\Delta x}$$
$$+\frac{\eta^*_{r+1,s+1}-\eta^*_{r-1,s+1}+\eta_{r+1,s}-\eta_{r-1,s}}{4\Delta x}$$
$$=\frac{1}{3}\frac{u_{r+1,s+1}-2u_{r,s+1}+u_{r-1,s+1}-u_{r+1,s}+2u_{r,s}-u_{r-1,s}}{\Delta x^2\Delta t}, \quad (6)$$

and (iii) the continuity equation for $\eta_{r,s+1}$ is

$$\frac{\eta_{r,s+1}-\eta_{r,s}}{\Delta t}+(1+\eta_{r,s})\frac{u_{r+1,s+1}-u_{r-1,s+1}+u_{r+1,s}-u_{r-1,s}}{4\Delta x}$$
$$+\tfrac{1}{2}(u_{r,s+1}+u_{r,s})\frac{\eta_{r+1,s}-\eta_{r-1,s}}{2\Delta x}=0. \qquad (7)$$

An estimate of the accuracy of these approximate equations was found by using the known solution for a solitary wave. A solitary wave of amplitude 0·1 was used as the initial condition in calculations with both I and II. The solution should have remained steady. With I the amplitude steadily decreased, the rate of decrease was less for smaller Δ, so Δ was chosen sufficiently small for the discrepancy to be no more than 5 % at the end of the integration. With II there was a small initial change in amplitude and then the wave profile was almost steady. The better convergence of II appears to be due to the truncation error in (6) being $O(\Delta^3\epsilon\delta^3)$, while it is only $O(\Delta^2\epsilon\delta^3)$ in (4).

The range of integration in x was advanced with unit velocity in order to reduce computation time. The usual range of integration in x was 45 and computation was usually continued up to $t = 80$.

4. Results

In most of the numerical calculations the initial wave-form was

$$u=\tfrac{1}{2}u_0[1-\tanh(x/a)] \quad \text{and} \quad \eta=u+\tfrac{1}{4}u^2. \qquad (8), (9)$$

The initial condition (8) alone was used for calculations with I. The value of η given by (9) is the one appropriate to Airy's theory. The value of a was chosen sufficiently large that the initial motion was described by Airy's theory. Since the equations are only correct for small amplitudes, u_0 was usually taken to be 0·2 or less. Even so, η almost reached 0·5 in calculations with $u_0 = 0{\cdot}2$.

The results of two representative calculations with I are shown in figures 3 and 4. The corresponding solutions of Airy's theory are given for comparison, and, as expected, the calculated solutions are close to it initially. The departure from Airy's theory and the growth of the undulations are seen to confirm the qualitative argument of § 2. After the first undulation appeared, its rate of growth was usually constant for a surprising length of time. This initial rate of growth varied with the square of the initial amplitude. This is illustrated in figure 5, which shows the maximum value of u plotted against time for a representative series of calculations: the scale for u is in terms of u_0^2.

It is clear that to some extent these results depend on the form of the initial wave. A calculation using a sine curve to join two level surfaces in the initial wave gave slightly different results. The difference was probably due to the transition between levels being more abrupt for a given maximum slope than with the hyperbolic tangent, and there was also a discontinuity in the second derivative where the sine curve joined the constant level. If the initial wave is relatively steep, the rate of growth of the first undulation is not constant but decreases slowly after a rapid start (e.g. figure 7). The velocity of the first crest was the same as that of a solitary wave of the same amplitude, $1+\frac{1}{2}a+O(\epsilon^2)$.

Both approximate equations I and II were used, and the solutions agreed to

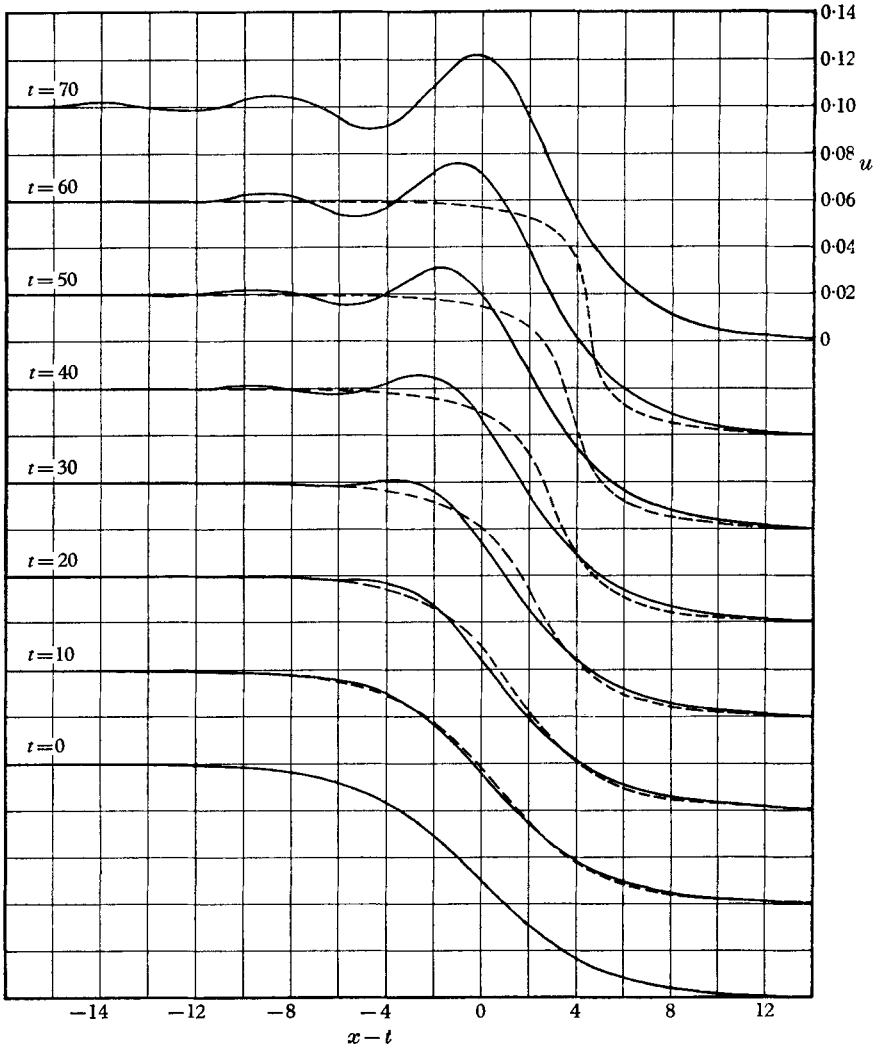

FIGURE 3. Initial growth of an undular bore, using I, with $\Delta = 0{\cdot}2$, $u_0 = 0{\cdot}1$, $a = 5$. The solution of Airy's theory is indicated by a dashed line.

within the errors in numerical approximation that were expected from the preliminary calculations (§ 3). That is, the solutions were very nearly the same near the start of an integration, but as it proceeded the solution from I steadily fell below that from II.

There are few published experimental results for the initial growth of undular bores with which these calculations can be compared. Favre (1935, figure 47, page 152) gives four profiles of equivalent waves at different times. These profiles indicate a rate of growth similar in magnitude to that calculated.

5. The fully developed undular bore

After some time, an undular bore reaches an almost steady state, and there are more experimental results for this condition (Favre 1935; Sandover & Zienkiewicz

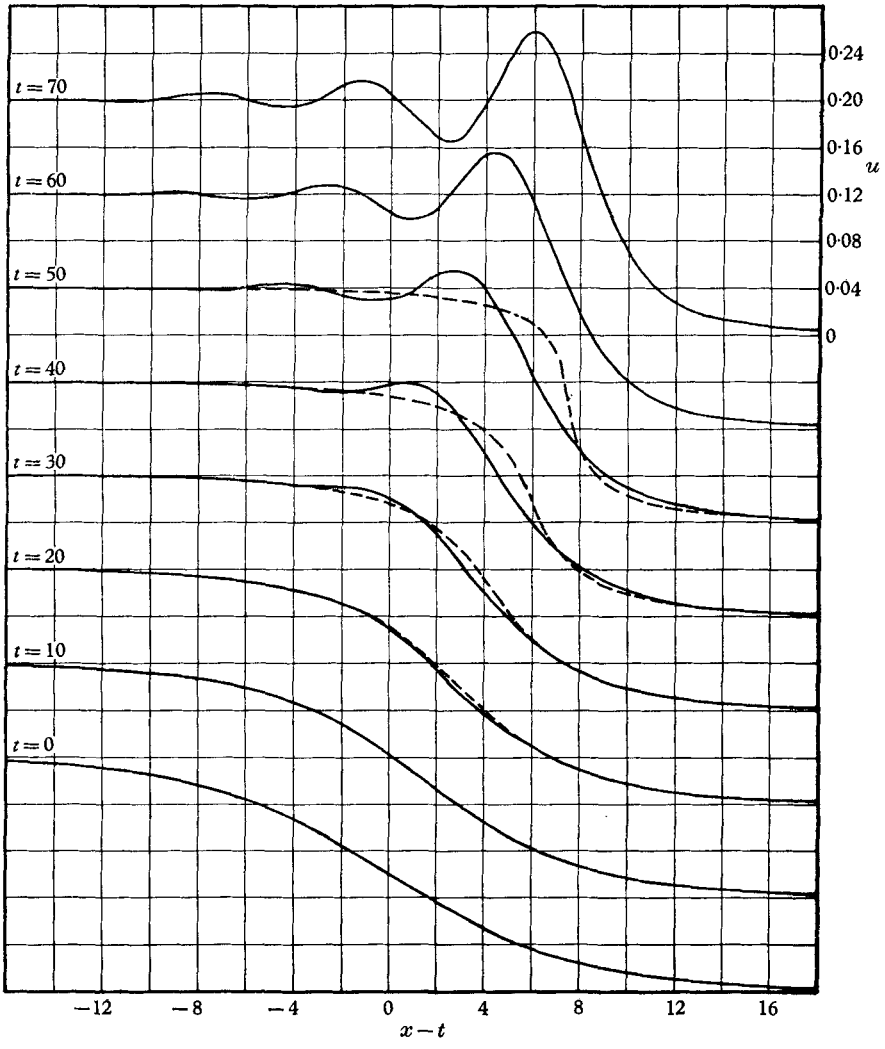

FIGURE 4. Initial growth of an undular bore, using I, with $\Delta = 0{\cdot}2$, $u_0 = 0{\cdot}2$, $a = 8$. The solution of Airy's theory is indicated by a dashed line.

1957; Sandover & Taylor 1962). Since the numerical approximation for II appeared to converge relatively well, some computations were extended to see how the results compared with experiment. An example is illustrated in figures 6, 7 and 8.

There is only one steady translational solution of the equations with still water in front of a wave, that is the solitary wave. In the experimentally observed steady state, there is an almost uniform train of waves at the head of the bore. Keulegan & Patterson (1940) showed that these waves behaved like cnoidal waves in Favre's experiments. Benjamin & Lighthill (1954) showed further that a uniform train of cnoidal waves can only form on a uniform flow if there is a change in the energy of the flow, and thus a uniform train of cnoidal waves cannot form an undular bore unless some frictional effects are present. The most

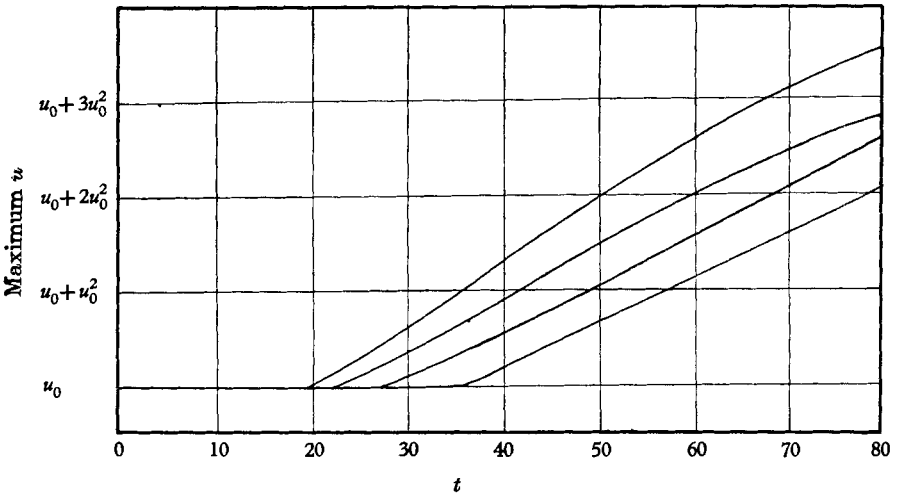

FIGURE 5. The maximum amplitude of u as a function of time. From left to right the curves are for $u_0 = 0{\cdot}2$, $0{\cdot}15$, $0{\cdot}1$, $0{\cdot}05$. The first is from equations II with $\Delta = 0{\cdot}25$, the others are from I with $\Delta = 0{\cdot}2$, and all have $a = 5$.

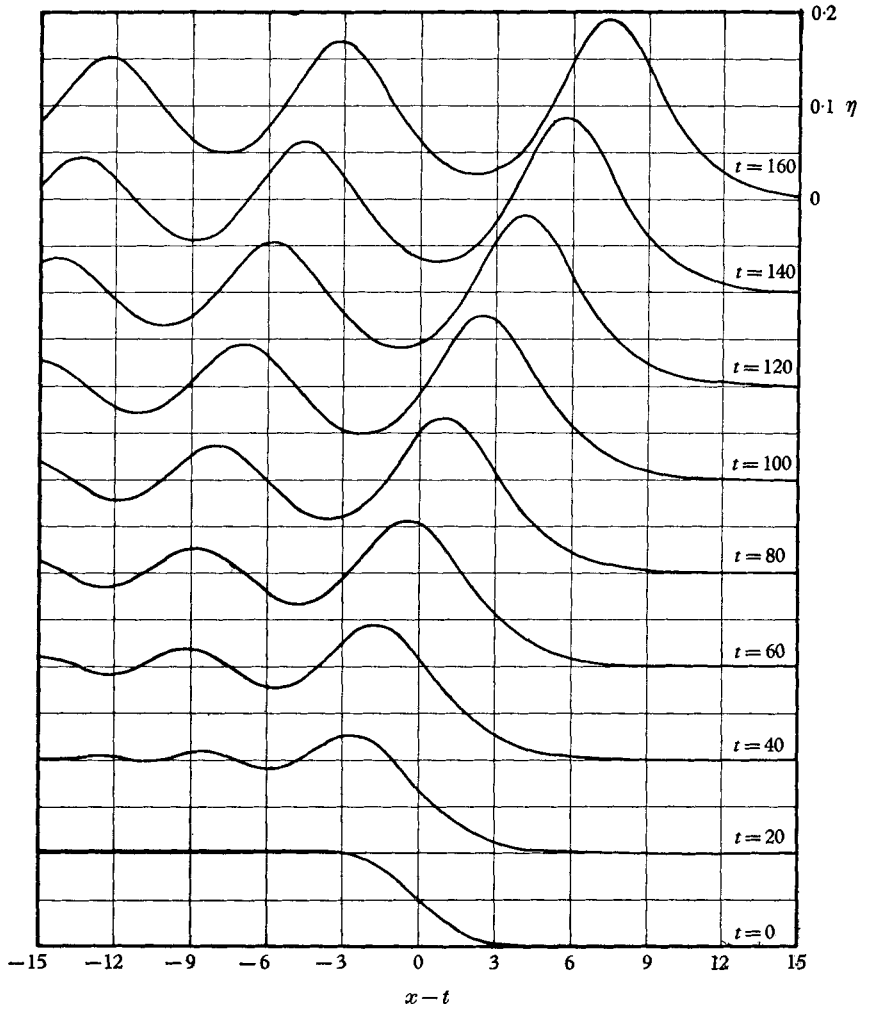

FIGURE 6. The growth of an undular bore, using II, with $u_0 = 0{\cdot}1$, $a = 2$, and $\Delta = 0{\cdot}25$.

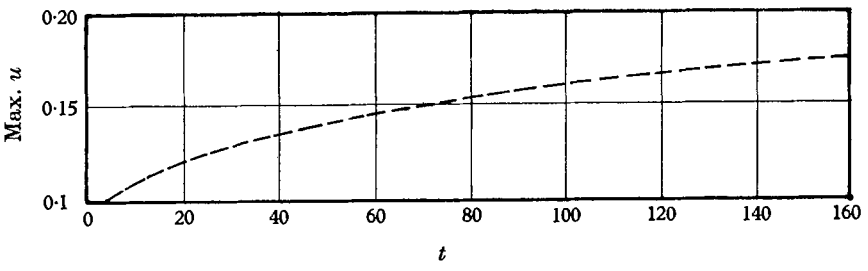

FIGURE 7. Maximum amplitude of u: the same calculations as figure 6.

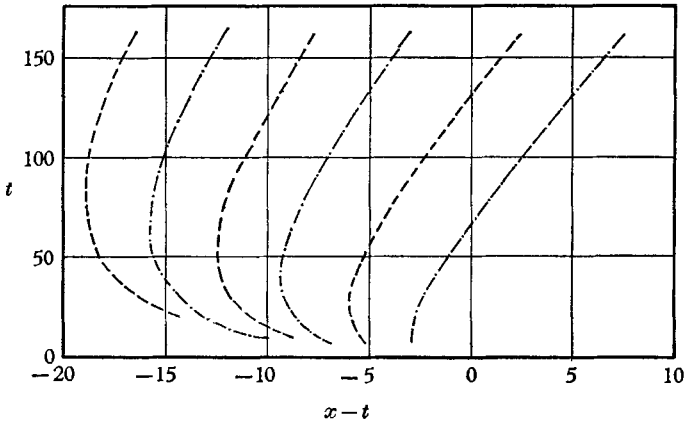

FIGURE 8. Position of crests and troughs: the same calculations as figure 6.
—·—·—·—, Crests; ————————, troughs.

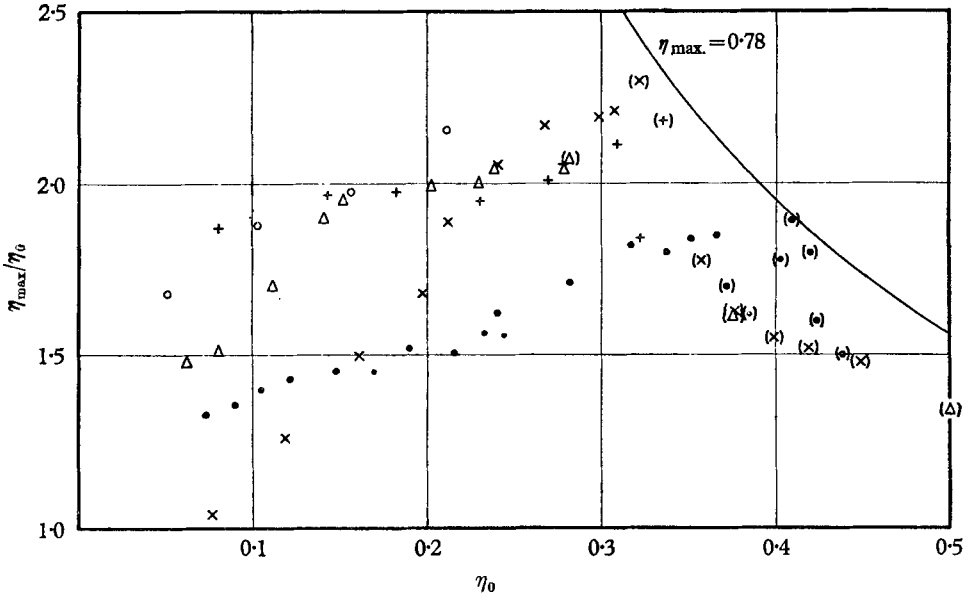

FIGURE 9. The maximum amplitudes of undular bores. ○, Calculations; △, Favre; ×, Sandover & Taylor (24 ft.); +, Sandover & Taylor (48 ft.); ●, Sandover & Zienkiewicz; ( ), indicates breaking.

likely behaviour for an idealized inviscid bore is that the leading waves slowly draw away from each other, so that the bore tends to become a succession of solitary waves. This hypothesis is supported by the result that two equal solitary waves travelling in the same direction gradually separate (Brooke Benjamin, personal communication). In the calculated results the profile of the first undulation agrees to the first order with that of a solitary wave of the same height.

The maximum amplitude attained by the undulations in the calculations is compared with the experimental results in figure 9. The marked discrepancy of Sandover & Zienkiewicz's results is probably due to their channel being smaller than the others and the effect of viscosity being more important. Some of the other measurements appear to have been taken before the maximum amplitude was reached. The calculated results are in general agreement with the experiments.

The maximum amplitude of the undulations is limited by breaking. The line corresponding to the solitary wave of maximum height is included in the diagram since it is likely that any undulation can only momentarily exceed that height without breaking. It is interesting to note that most of the measured breaking waves have an amplitude of about 0·6. The small-amplitude approximation used here is clearly not relevant to these finite-amplitude effects. The length of the first wave in the calculated bores is in good agreement with Favre's measurements.

In practice, undular bores are influenced by viscosity, most usually through interactions with a turbulent flow. No attempt has been made to include the effect of viscosity in these calculations. If empirical terms to represent dissipation are included, a steady profile may be found by integrating an ordinary differential equation; both Sandover & Taylor, and Sandover & Zienkiewicz show the results of such an integration.

I wish to thank the Department of Scientific and Industrial Research for a studentship, the Director of the University Mathematical Laboratory, Cambridge, for permission to use EDSAC II for the computations, and Dr T. Brooke Benjamin for helpful discussions in the course of this work.

REFERENCES

BENJAMIN, T. B. & LIGHTHILL, M. J. 1954 On cnoidal waves and bores. *Proc. Roy. Soc.* A, **224**, 448–60.

BINNIE, A. M. & ORKNEY, J. C. 1955 Experiments on the flow of water from a reservoir through an open channel. II. The formation of hydraulic jumps. *Proc. Roy. Soc.* A, **230**, 237–46.

BROER, L. J. F. 1964 *Appl. Sci. Res.* B, **11**, 273–85.

FAVRE, H. 1935 *Ondes de Translation.* Paris: Dunod.

KEULEGAN, G. H. & PATTERSON, G. W. 1940 Mathematical theory of irrotational translation waves. *Nat. Bur. Standards J. Res.* **24**, 47–101.

KORTEWEG, D. J. & DE VRIES, G. 1895 *Phil. Mag.* (V), **39**, 422–43.

LONG, R. R. 1964 *J. Fluid Mech.* **20**, 161–70.

SANDOVER, J. A. & TAYLOR, C. 1962 *La Houille Blanche*, **17**, 443–55.

SANDOVER, J. A. & ZIENKIEWICZ, O. C. 1957 Experiments on surge waves. *Water Power*, **9**, 418–24.

STOKER, J. J. 1957 *Water Waves.* New York: Interscience.